

TEMPORAL AND SPATIAL DISTRIBUTION OF SEASONAL CO₂ SNOW AND ICE. T. N. Titus¹ and H. Kieffer¹, ¹ U.S. Geological Survey, 2255 North Gemini Dr., Flagstaff, AZ 86001.

Introduction: The seasonal polar caps are a major element of Mars' climate and global atmospheric circulation. Theoretical calculations [1,2] and surface pressure measurements [3] indicate that about ¼ of the CO₂ in the atmosphere condenses each year to form the seasonal caps. Changes in the polar cap albedo or emissivity modify the polar cap energy budget and the amount of CO₂ condensation, consequently affecting the global martian climate.

Variations in both albedo and emissivity have been observed by several spacecraft. In the 1970s, spacecraft observations of the polar regions of Mars revealed polar brightness temperatures that were significantly below the expected kinetic temperatures (140 - 148 K) for CO₂ in sublimation equilibrium with the martian atmosphere [4]. The observational footprints were typically a few hundred kilometers in diameter, with 20 μm brightness temperatures (T₂₀) as low as 130 K and had characteristic durations of a few days [4]. For historical reasons, we will refer to these regions as cold spots even though more recent observations [5, 6, 7] support their kinetic temperatures being the same as the rest of the polar cap. A general lack of correlation between cold spots and Mars Global Surveyor (MGS) Mars Orbiter Laser Altimeter (MOLA) measurements of clouds and Thermal Emission Spectrometer (TES) spectra suggest that most of the cold spots are surface regions of low emissivity. Occasionally, there are correlations to extremely dense polar night clouds and the "coldest" of the cold spots, suggesting a few of these cold spots may be "dry ice blizzards" in progress [6].

The MGS TES observations, combined with spectral modeling [5,7] using new CO₂ optical constants [8], illustrate that the "cold spots" are due to fine-grain CO₂, which cause a decrease in the 25 μm emissivity. Spectral models predict that fine-grain CO₂ (hereafter referred to as snow, regardless of the formation process) has high albedo and low emissivity in the 25-μm-transparency band. Coarse-grained CO₂ (hereafter referred to as ice) has low albedo (perhaps even transparent if the dust content is low) and near unit emissivity. Increasing the dust content in the CO₂ results in a large decrease in albedo, but only a slight increase in emissivity. TES observations have shown these effects [9] for the southern springtime season cap, suggesting that the bright outliers (e.g. the Mountains of Mitchel) are snow covered, while other areas (e.g. the cryptic region) are mainly composed of ice.

The purpose of this paper is to present results from the MGS TES continuing mission, showing the distribution of CO₂ snow and ice in space and time. The dense coverage of the Mars polar regions by MGS TES has provided the ability to monitor the seasonal variations of condensates. Because TES has three subsystems, we can monitor the distribution of solid CO₂ in two ways: (1) monitoring the spectral differentiation between snow and ice and (2) the estimation of local CO₂ mass accumulation.

The TES solar bolometer, combined with synthetically derived brightness temperatures, can differentiate between snow and ice [9]. The difference between the estimated surface kinetic temperature, T₁₈, and the brightness temperature in the CO₂ 25 μm transparency band, T₂₅, effectively measures the emissivity at 25 μm and is taken as an indicator of the grain size of CO₂ frost [5,6,9]. We will use the same convention as Titus et al. [6] where ice is defined as $\Delta T = T_{18} - T_{25} < 5$ K. This measure can be influenced by the presence of atmospheric dust, however that effect has not yet been quantified.

The TES directly measures the total reflected and emitted radiation, which in turn allow for the measurement of the geographic variation of the net radiation balance and, through integration of the inferred sublimation rates, the annual solid CO₂ budget. We use the sublimation budget instead of the condensation budget to minimize the impact of lateral transport of heat during the polar night [5, 10]

Data: The MGS spacecraft orbit has an inclination of 93°, ascending (going north) on the night-side and going south (descending) on the dayside with a 14-hour Mars local time (H) equator crossing. For simplicity, we will refer to TES observations acquired on the ascending leg as AM and those acquired on the descending leg as PM. In normal mapping nadir-oriented mode, TES sweeps a 9 km wide swath along the sub-spacecraft track, which is almost parallel to meridians except near the pole. In this observation mode, the times between repeat coverage is highly dependent on latitude, ranging from only a few hours along the "polar rings" at ± 87° latitude to several days at ± 60° latitude. This allows detailed analysis of spatial and temporal changes near the polar caps. However, at more equatorial latitudes seasonal analysis of specific locations is restricted due to the lengthy repeat time, approaching hundreds of days near the equator.

The TES data used were binned spatially into a polar stereographic projection with a mean resolution of 60 km per cell. Temporal binning was done on a base of 12 orbits (approx 23.55 hours). Missing data in the latitude/season cells were filled by linear interpolation in time.

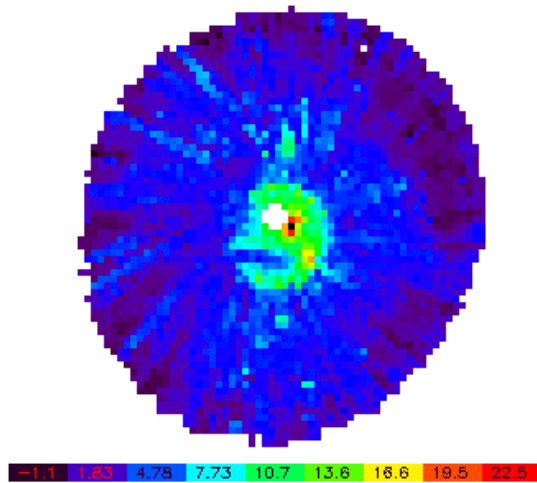


Figure 1: North polar grain-size index, ΔT , at $L_s = 342^\circ$. All polar figures have the same scale where the outer limits are at 45° latitude. The white plus in the center of the image is pole. Areas off the polar cap are white.

Snow and Ice Distribution:

North Polar Distribution. The winter (or condensation phase) cap is generally characterized by the observed $25 \mu\text{m}$ brightness temperatures (T_{25}) near the expected surface temperatures for solid CO_2 , suggesting that direct surface condensation as slab ice occurs. Kieffer and Titus [5] and Titus et al. [6] show that cold spot observations, strong indicators of snow, are restricted to the perennial cap and other localized topographical features, e.g. craters. We conducted a space-time analysis; our latest analysis is consistent with these prior results. The perennial cap has a high frequency of cold spot occurrence from approximately at $L_s = 200^\circ$ to approximately at $L_s = 350^\circ$.

The springtime (or sublimation phase) cap is generally characterized by low ΔT , suggesting slab ice. However, by $L_s = 45^\circ$ a bright ring has formed just inside the receding cap edge. [Fig. 2] This bright ring is not visible in the ΔT image, suggesting that the brightening is not due to CO_2 grain size effects. One plausible source of this bright receding ring is that water released from the season cap edge is redeposited as frost inside the cap [11].

During this same period of time, the perennial cap also appears bright without a corresponding increase in ΔT .

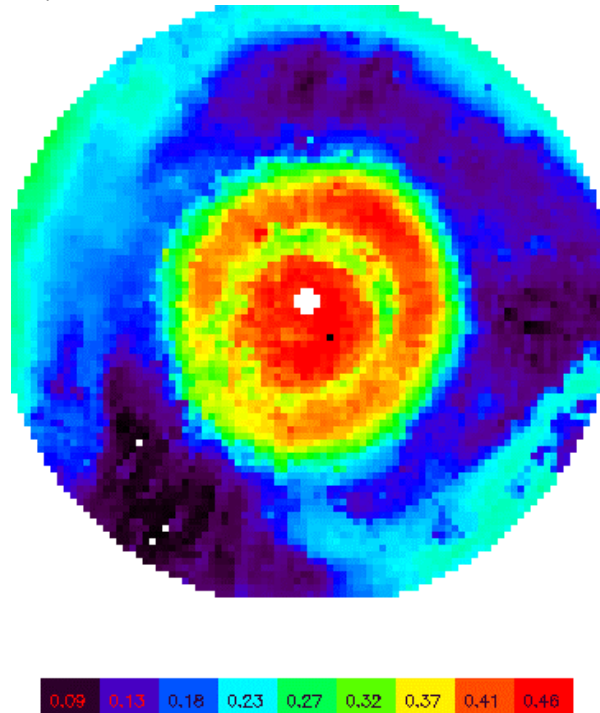


Figure 2: North polar cap albedo and grain-size index at $L_s=38^\circ$. There is a lack of correlation between these two parameters, suggesting that the brightening of the cap is due to water frost, not fracturing of CO_2 .

South Polar distribution: Cold spot activity in the southern winter starts approximately $L_s=16^\circ$. The Mountains of Mitchel is one of the most active regions. Cold spot activity continues until approximately $L_s=150^\circ$. After the sun has risen above the horizon, the cap begins to brighten, with the areas closest to the edge brightening first. A similar effect is

seen in ΔT , suggesting that the albedo brightening is due to an effective grain-size of the surface CO_2 grain-size. Paige [12] explained this phenomenon as the fracturing of the surface ice due to insolation. TES observations are consistent with this explanation.

In many cases, the brightest springtime regions were areas of greatest winter cold spot activity. Perhaps wintertime accumulation of snow increases the likelihood that fracturing occurs in the spring.

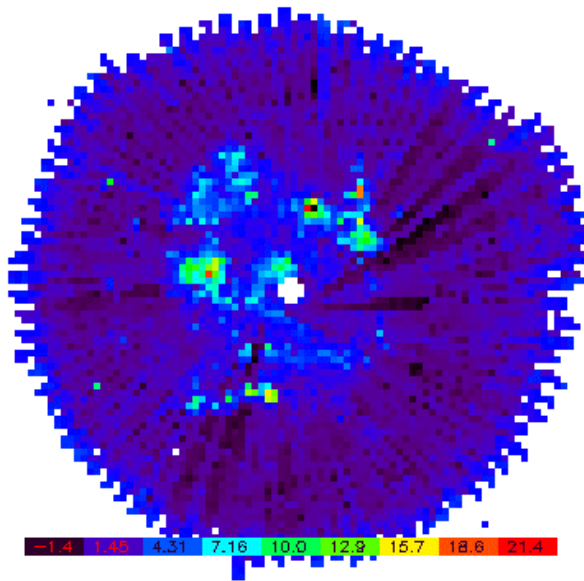


Figure 3: South polar cap grain-size index at $L_s=86^\circ$. The Mountains of Mitchel is one of the areas with high ΔT , suggesting the presence of snow.

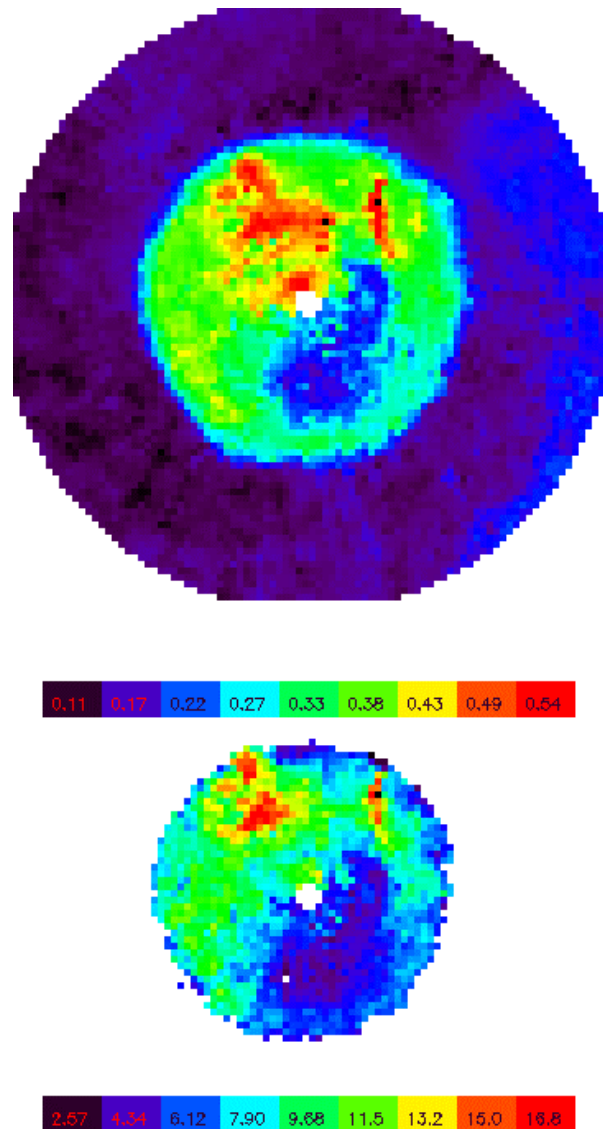


Figure 4: South polar albedo and grain-size index at $L_s=217^\circ$. Bright albedo areas generally have high ΔT , while areas with low albedo tend to have low ΔT .

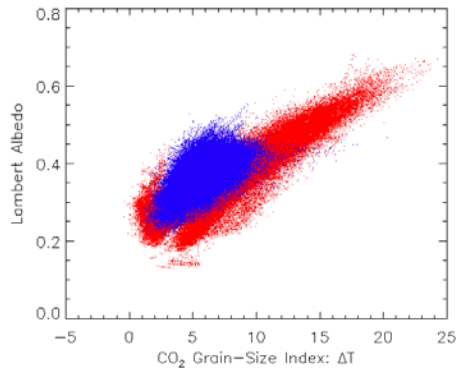


Figure 5: Albedo vs. CO₂ grain-size index. The data were restricted to springtime data with surface temperature less than 160 K. The red dots are for the south polar cap and the blue dots are for the northern polar cap.

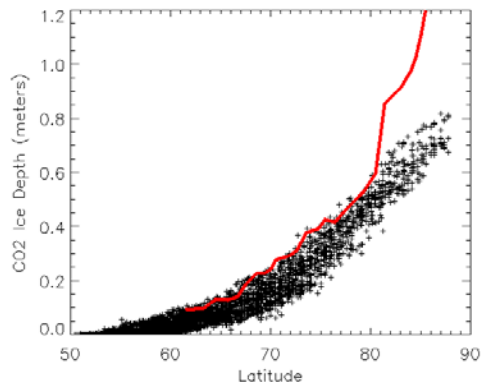


Figure 6: North polar seasonal cap depth estimates. The black pluses are seasonal cap depths estimated from TES mass-balance calculations, assuming a CO₂ density of 1606 kg/m³. The red line is an estimate from MOLA.

CO₂ Mass Budget: The underlying assumptions in the TES mass balance calculations are that the total energy input into Mars is characterized by the solar bolometer and that the total energy out of the Mars system is characterized by the thermal bolometer. The energy difference between the input and output is assumed to be due to the sublimation or condensation of CO₂. This implies that there is no geothermal heating or lateral transport of heat through the atmosphere. While initial estimates suggest that geothermal heating is negligible, a comparison of condensation and sublimation mass budgets suggest that a large amount of heat transport does occur during the polar night [5,10]. However, comparisons of the sublimation budget to other observations [13] suggest that this technique is a

good estimate of actual amount of CO₂ in the springtime seasonal caps. For a detailed description of how the mass balance calculation is done, see Kieffer et al. [5] Figure 6 shows the estimated depth of seasonal CO₂ if one assumes a pure substance ($\rho = 1606 \text{ kg/m}^3$) compared to the seasonal depth estimated by MOLA [13]. If one assumes that the MOLA estimates are correct, we estimate the density of ice (latitudes south of 80°N) as $1107 \pm 150 \text{ kg/m}^3$ and the density of snow/ice mixture (latitudes north of 80°N) as $979 \pm 133 \text{ kg/m}^3$. The south polar MOLA depth estimates are not presented here because of possible systematic errors in their depth estimates. When comparing MOLA and TES estimates, this offset must be $\sim 20 \text{ cm}$ to bring southern density estimates into agreement with the density for northern ice. A 20 cm offset is consistent with possible systematic errors for the southern data [14]. While these density estimates are preliminary, they are consistent with TES spectral observations of snow and ice distributions.

Conclusions:

- The predominate form of CO₂ condensation is direct surface condensation as slab ice.
- Regions with a high frequency of snow deposition during the winter generally have brighter than average albedo in the spring, e.g. the Mountains of Mitchel.
- Springtime brightening of the south polar cap is predominately a change in grain size of the CO₂. This is not the case for receding northern cap. Albedo variations are most likely dominated by the presence of water frost.
- An estimate of martian northern CO₂ ice and snow/ice mixture densities based on combining TES mass balance calculations and MOLA seasonal elevation changes are $1107 \pm 150 \text{ kg/m}^3$ and $979 \pm 133 \text{ kg/m}^3$, respectively.

References:

- [1] Leighton R. and Murry B. (1966) *Sci.*, 153, 136-144. [2] Forget F. and Pollack J. (1996) *JGR*, 101, 16865-16879. [3] Tillman J. et al. (1993) *JGR*, 98, 10963-10971. [4] Kieffer H. et al. (1976) *Sci.*, 193, 780-786. [5] Kieffer H. and Titus T. (2001) *Icarus*, 154, 162-180. [6] Titus T. et al. (2001) *JGR*, 106, 23181-23196. [7] Hansen G. (1999) *JGR*, 104, 16471-16486. [8] Hansen G. (1997), *JGR*, 102, 21569. [9] Kieffer H. et al. (2000) *JGR*, 105, 9653-9699. [10] Titus T. (2003) *Mars Atm. Workshop*, Granada, Spain. [11] Kieffer H. (2002) *AGU Fall Mtg.*, Abstract P72C-02. [12] Paige D. (1985), *PhD Thesis*. [13] Smith D. et al. (2001) *Sci.*, 294, 2141-2146. [14] Smith D. *Personal communication*.